ETH zürich

Soot Size Distribution & Structure During Enclosed Spray Combustion of Jet Fuel

Una Trivanovic, Georgios A. Kelesidis, Sotiris E. Pratsinis

Particle Technology Laboratory, ETH Zürich, Switzerland

PTL Particle Technology Laboratory

FNSNF
Fonds national suisse
Schweizerischer Nationalfonds
Fondo nazionale svizzero
Swiss National Science Foundation

Aircraft emissions

Non-CO_2 radiative forcing accounts for 66% of aviation net radiative forcing! [1]

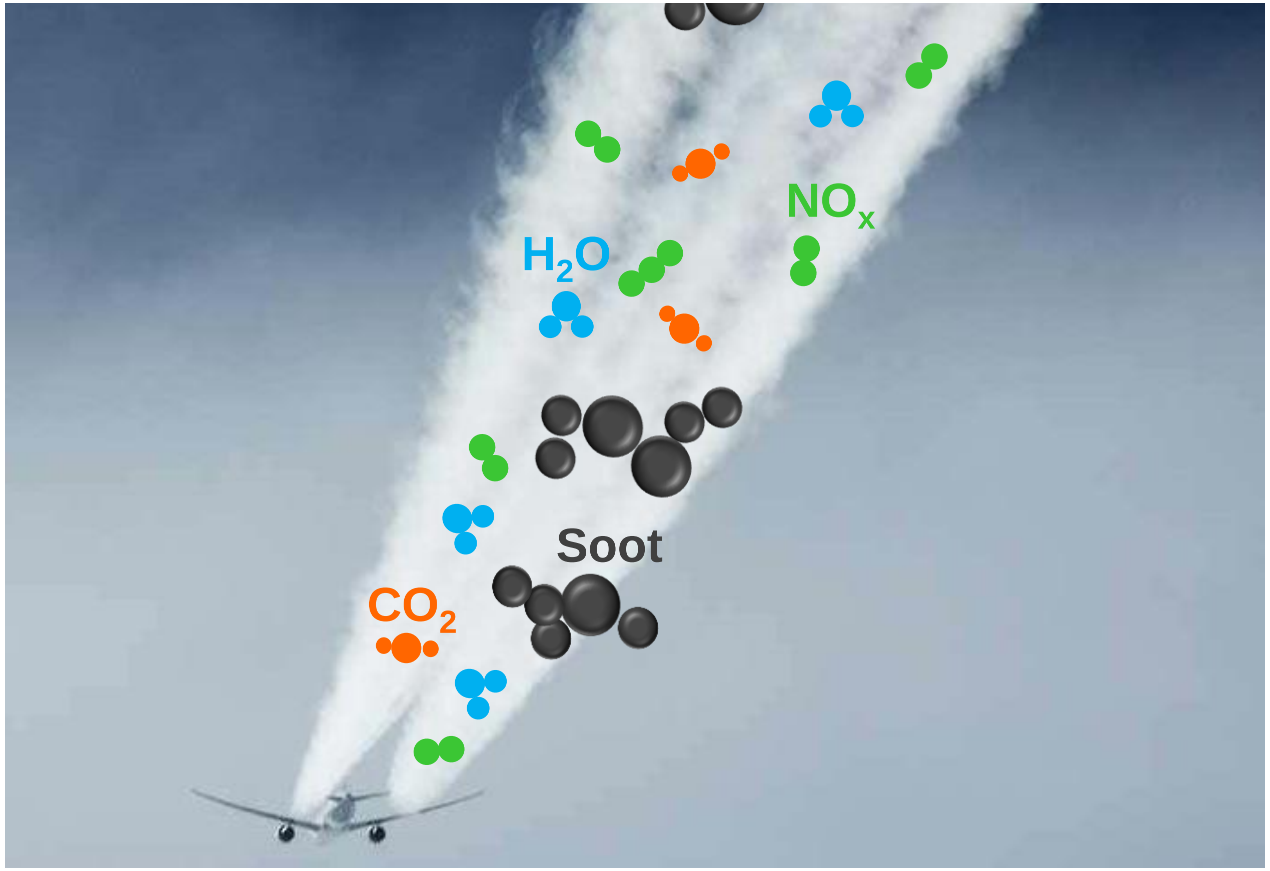

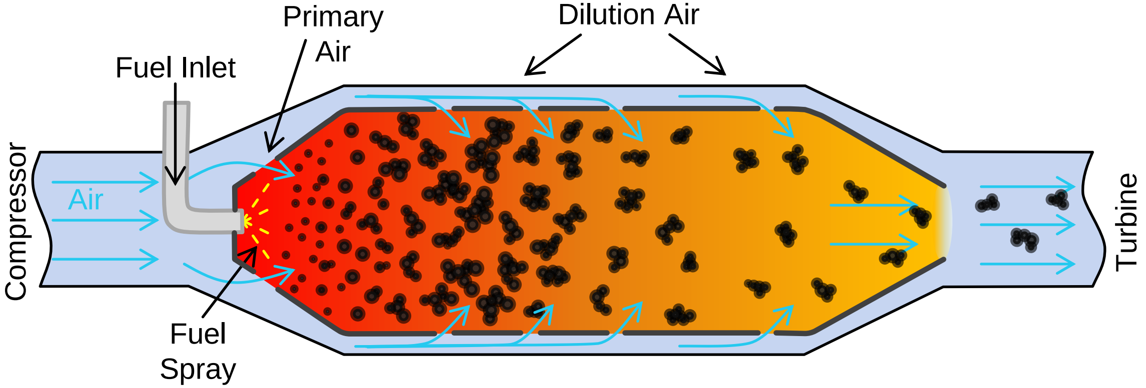

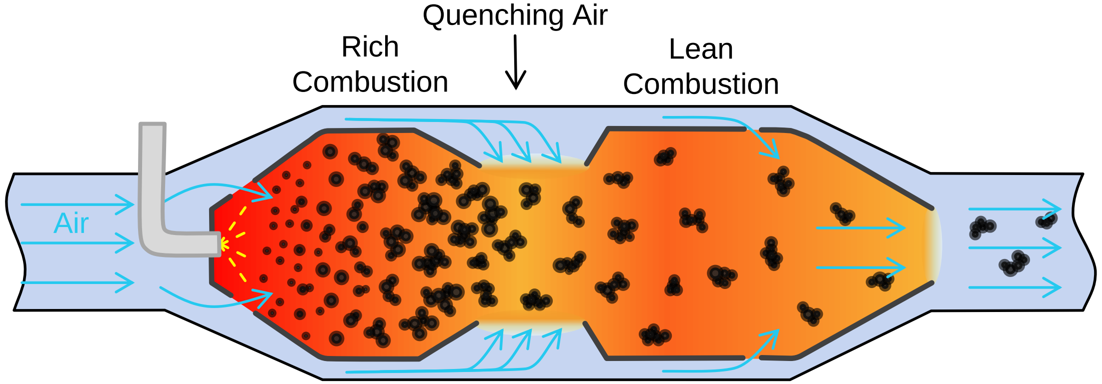

Combustion II: Poster 2CO.7 today at 1pm Exhibit Hall E

[1] Lee, D.S. et al. The contribution of global aviation to anthropogenic climate forcking for 2000 – 2018 (2021) *Atmos. Environ.* 244. 117834

[2] D. Westerdahl, S.A. Fruin, P.L. Fine, C. Sioutas (2008) *Atmos. Environ.* 42, 3143–3155.

Soot Generator

Enclosed spray combustion (ESC):

Aircraft-like with high throughput

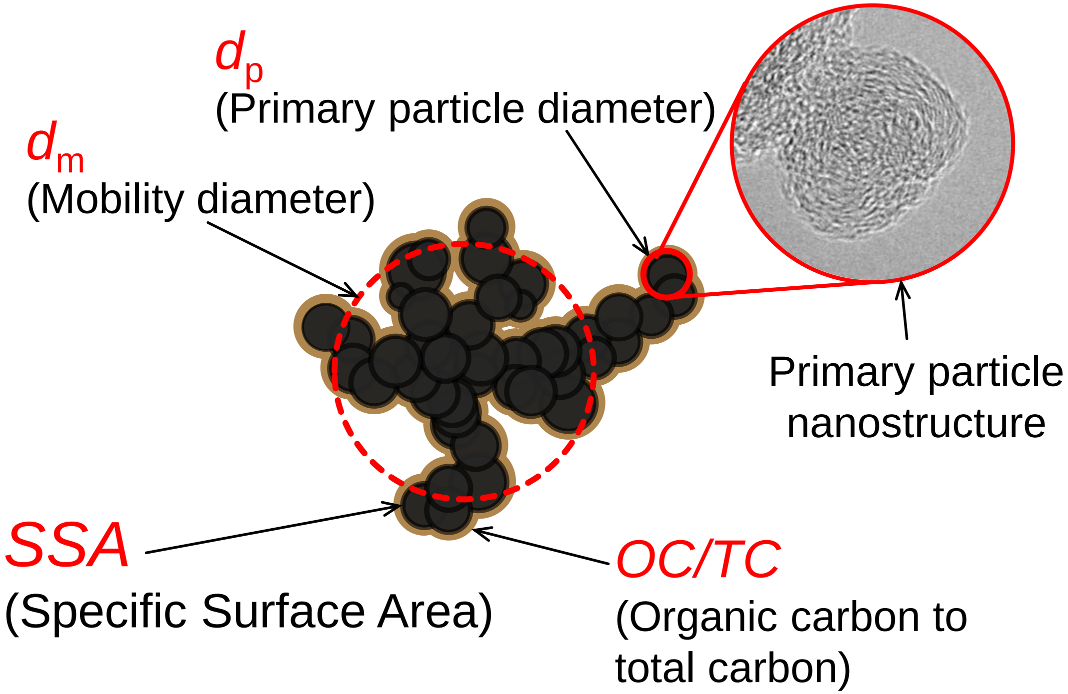

SSA measurements require 10s of mg of soot!

ESC Properties:

Median d_m = 15 – 170 nm

Median d_p = 12 – 23 nm

OC/TC = 10 – 20%

Raman D/G = 0.80 – 0.90

High-thrust Aircraft Soot Properties:

Median d_m = 11 – 60 nm [2, 3]

Median d_p = 10 – 20 nm [4]

OC/TC < 25% [5]

Raman D/G = 0.85 – 0.94 [6]

[1] U. Trivanovic, G.K. Kelesidis, S.E. Pratsinis (2022) *Aerosol Sci. Technol.* 56, 732-743.
[2] A.M. Boies *et al*. (2015) *Aerosol Sci. Technol.* 49, 842-855.
[3] M. Abegglen, L. Durdina, B.T. Brem, J. Wang, T. Rindlisbacher, J.C. Corbin, U. Lohmann, B. Sierau (2015) *J. Aerosol Sci.* 88, 135-147.
[4] A. Liati, B.T. Brem, L. Durdina, M. Vögtli, Y.A.R. Dasilva, P.D. Eggenschwiler, J. Wang (2014) *Environ. Sci. Technol. 48*, 10975 – 10983.
[5] D. Delhaye, F.-X. Ouf, D. Ferry, I.K. Ortega, O. Penanhoat, S. Peillon, F. Salm, X. Vancassel, C. Focsa, C. Irimiea, et al. (2017) *J. Aerosol Sci.* 105, 48 – 63.
[6] P. Parent, C. Laffon, I. Marhaba, D. Ferry, T.Z. Regier, I.K. Ortega, B. Chazallon, Y. Carpentier, C. Forsca (2016) *Carbon.* 101, 86 – 100

Enclosed spray combustion of jet fuel

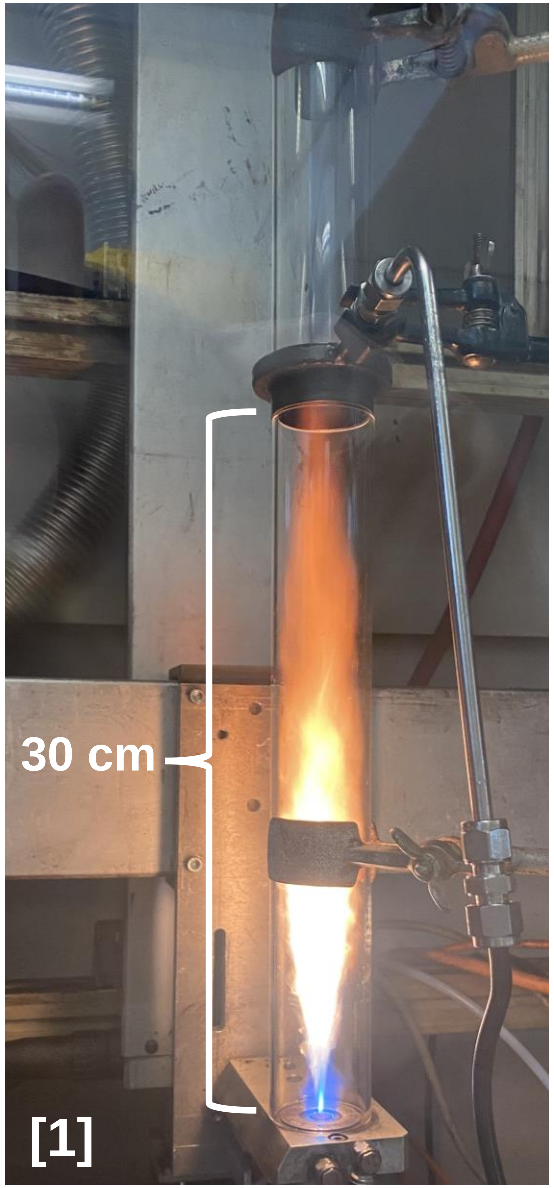

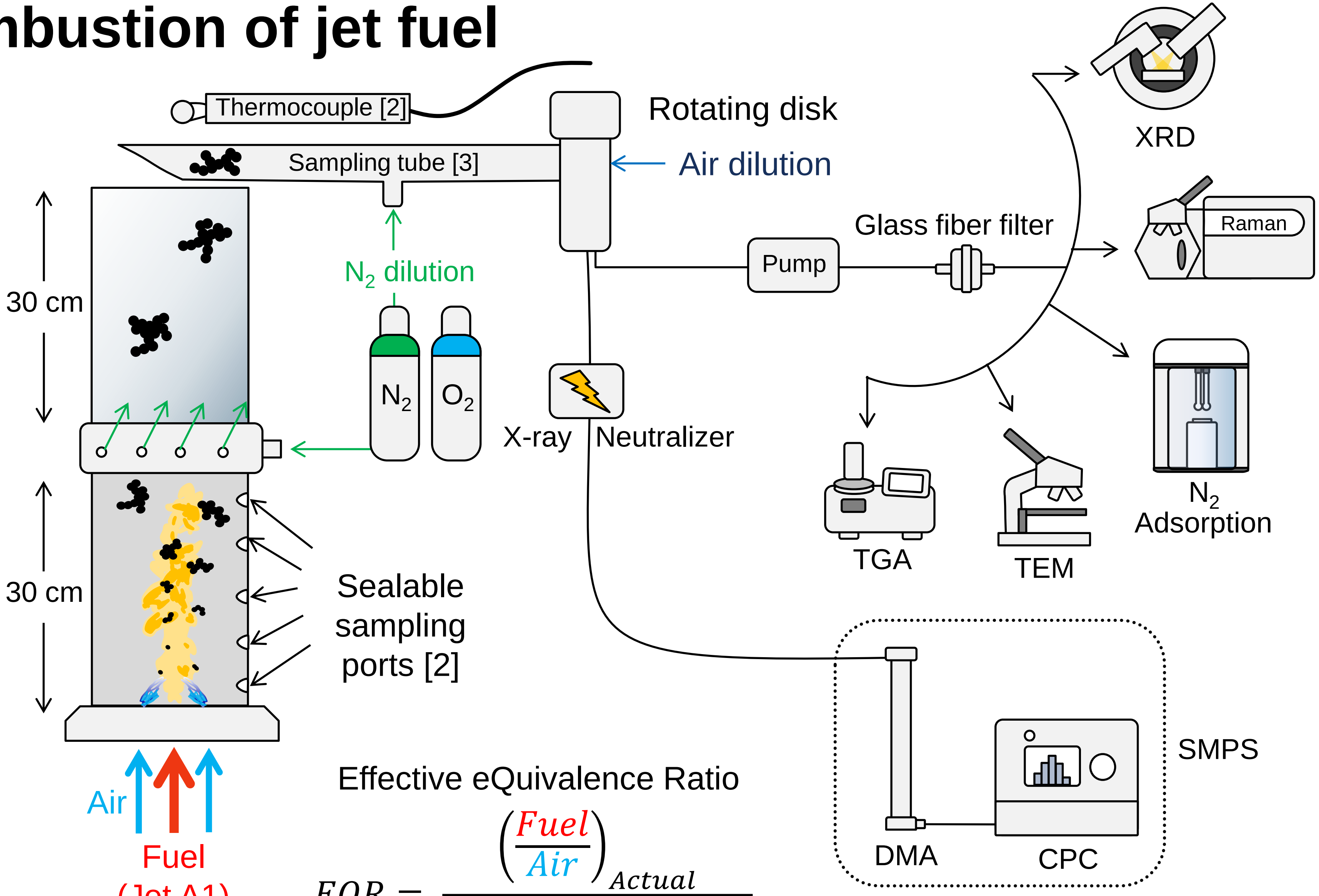

Effective eQuivalence Ratio

$$EQR = \frac{\left(\frac{Fuel}{Air}\right)_{Actual}}{\left(\frac{Fuel}{Air}\right)_{Stoichiometric}}$$

[1] U. Trivanovic, G.K. Kelesidis, S.E. Pratsinis (2022) *Aerosol Sci. Technol.* 56, 732-743.
[2] U. Trivanovic, M. Pereira Martins, S. Benz, G.A. Kelesidis, S.E. Pratsinis (2023) *Fuel.* 342, 127864.
[3] E. Goudeli, A. J. Gröhn, S.E. Pratsinis. (2016) *Aerosol Sci. Technol.* 50, 591-604.

Mass concentration

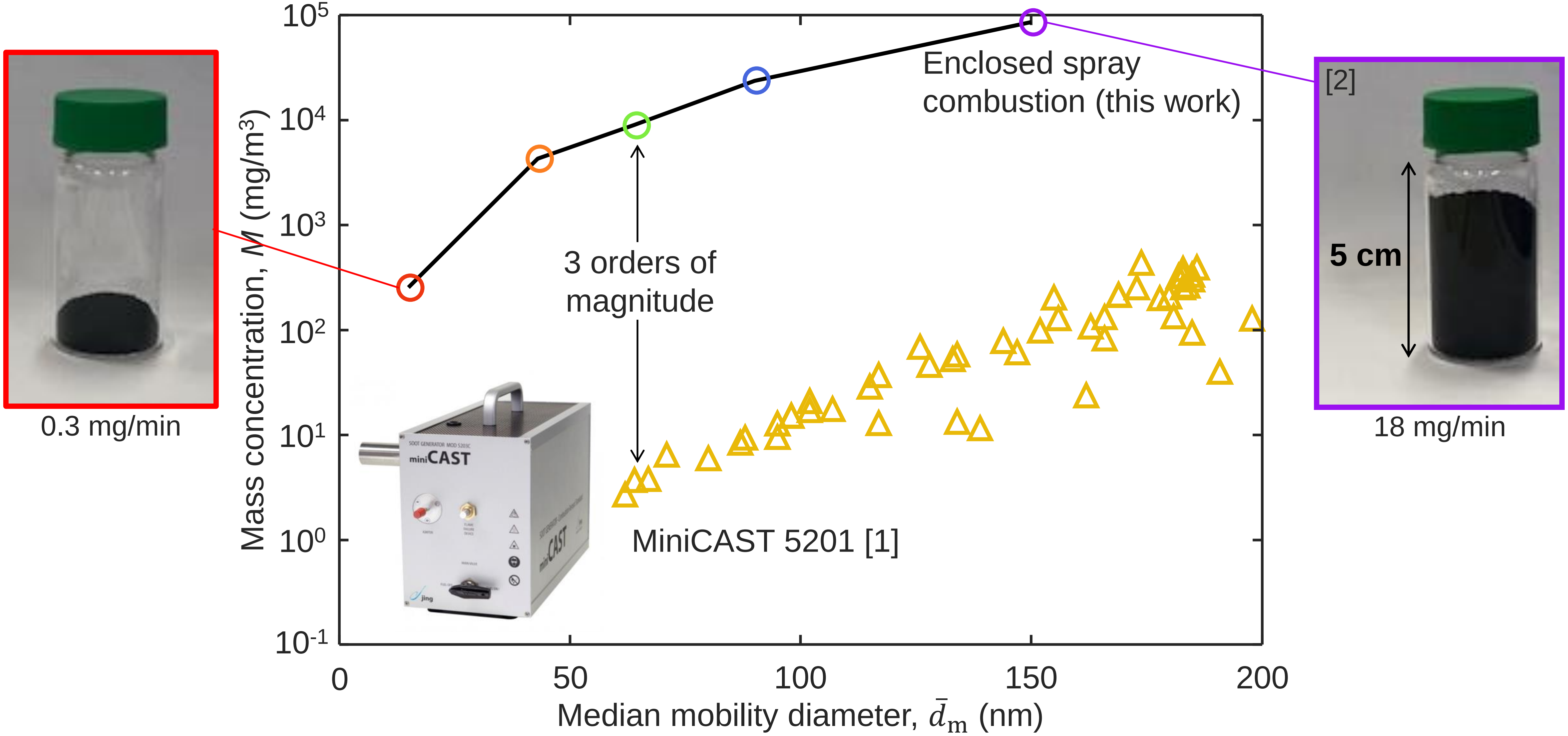

[1] M. Ess & K. Vasilatou (2019) *Aerosol Sci. Technol.* 53, 29 – 44.

[2] U. Trivanovic, G.K. Kelesidis, S.E. Pratsinis (2022) *Aerosol Sol. Technol.* 56, 732-743.

Pore size distributions & Specific Surface Area (*SSA*)

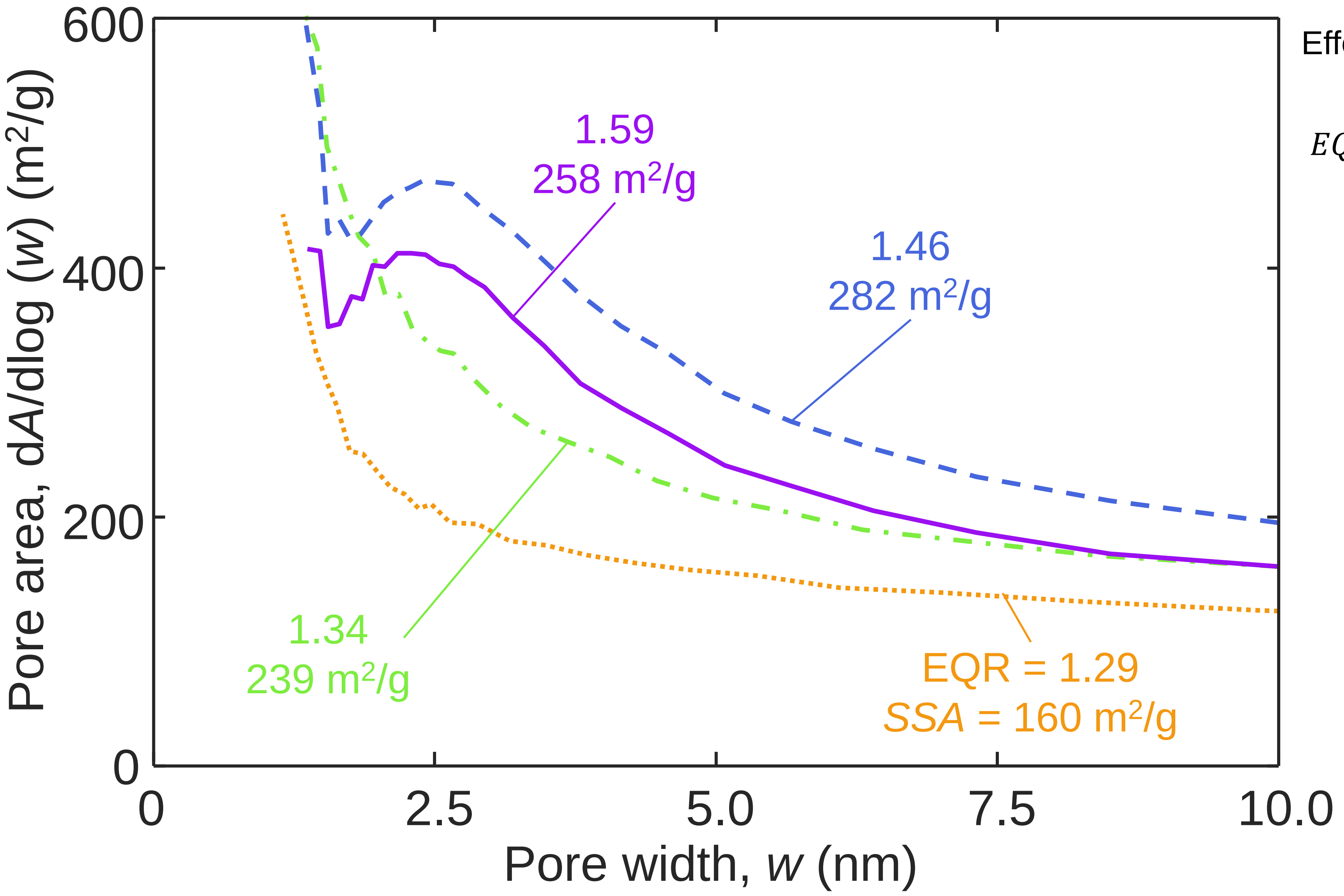

Effective eQuivalence Ratio:

$$EQR = \frac{\left(\frac{Fuel}{Air}\right)_{Actual}}{\left(\frac{Fuel}{Air}\right)_{Stoichiometric}}$$

Dynamics of soot d_m and d_p

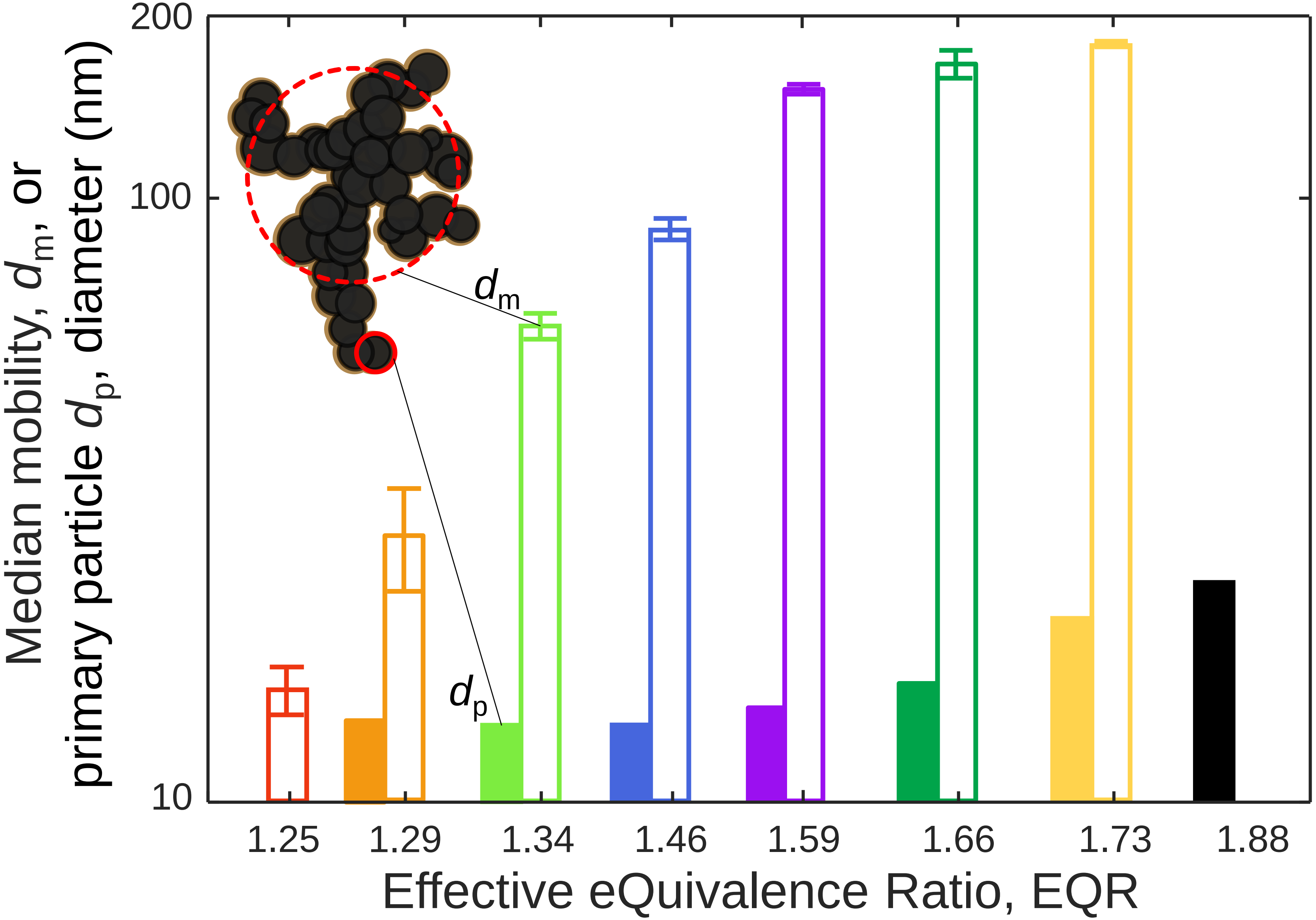

$$EQR = \frac{\left(\frac{Fuel}{Air}\right)_{Actual}}{\left(\frac{Fuel}{Air}\right)_{Stoichiometric}}$$

[1] A.M. Boies, M.E.J. Stettler, J.J. Swanson, T.J. Johnson, J.S. Olfert, M. Johnson, M.L. Eggersdorfer, T. Rindlisbacher, et al. (2015) *Aerosol Sci. Technol. 49*, 842 – 855.
[2] A. Liati, B.T. Brem, L. Durdina, M. Vögtli, Y.A.R. Dasilva, P.D. Eggenschwiler, J. Wang (2014) *Environ. Sci. Technol. 48*, 10975 – 10983.

Evolution of mobility and primary particle diameter (EQR = 1.46)

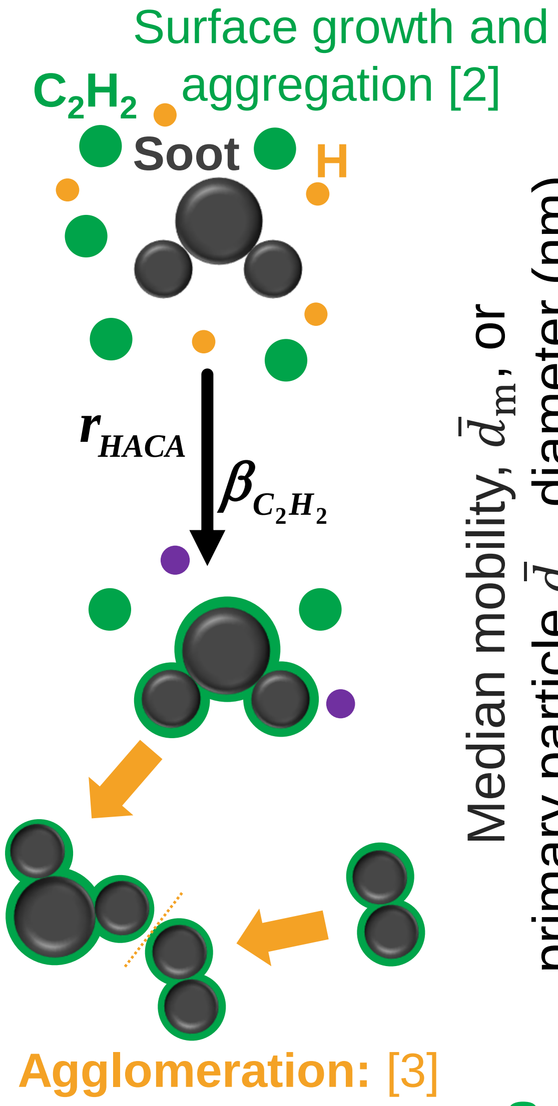

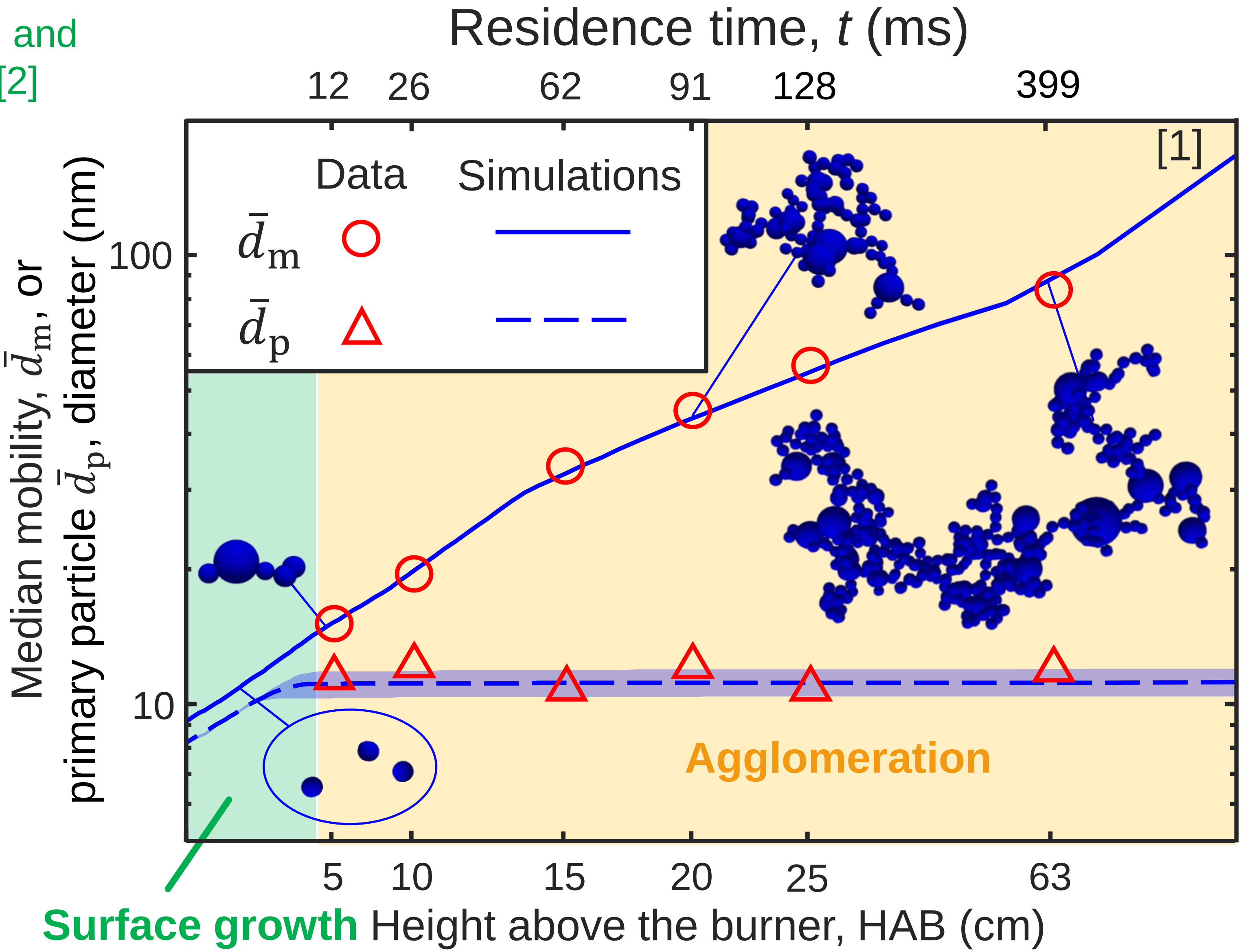

Effective eQuivalence Ratio:

$$EQR = \frac{\left(\frac{Fuel}{Air}\right)_{Actual}}{\left(\frac{Fuel}{Air}\right)_{Stoichiometric}}$$

[1] U. Trivanovic, M. Pereira Martins, S. Benz, G.A. Kelesidis, S.E. Pratsinis (2023) *Fuel.* 342, 127864.

[2] G.A. Kelesidis, E. Goudeli, S.E. Pratsinis (2017) *Proc. Combust. Inst.* 36, 29-50.

[3] G.A. Kelesidis, E. Goudeli, S.E. Pratsinis (2017) *Carbon.* 121, 527-535.

Raman vs Height Above the Burner (HAB)

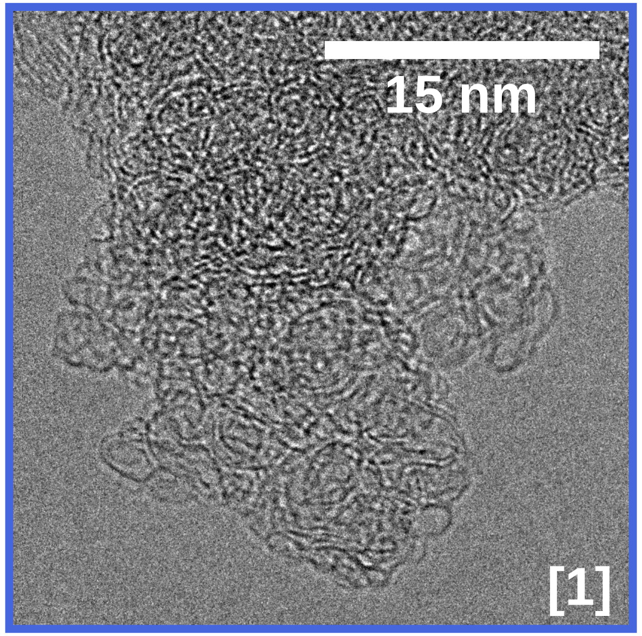

$$EQR = \frac{\left(\frac{Fuel}{Air}\right)_{Actual}}{\left(\frac{Fuel}{Air}\right)_{Stoichiometric}}$$

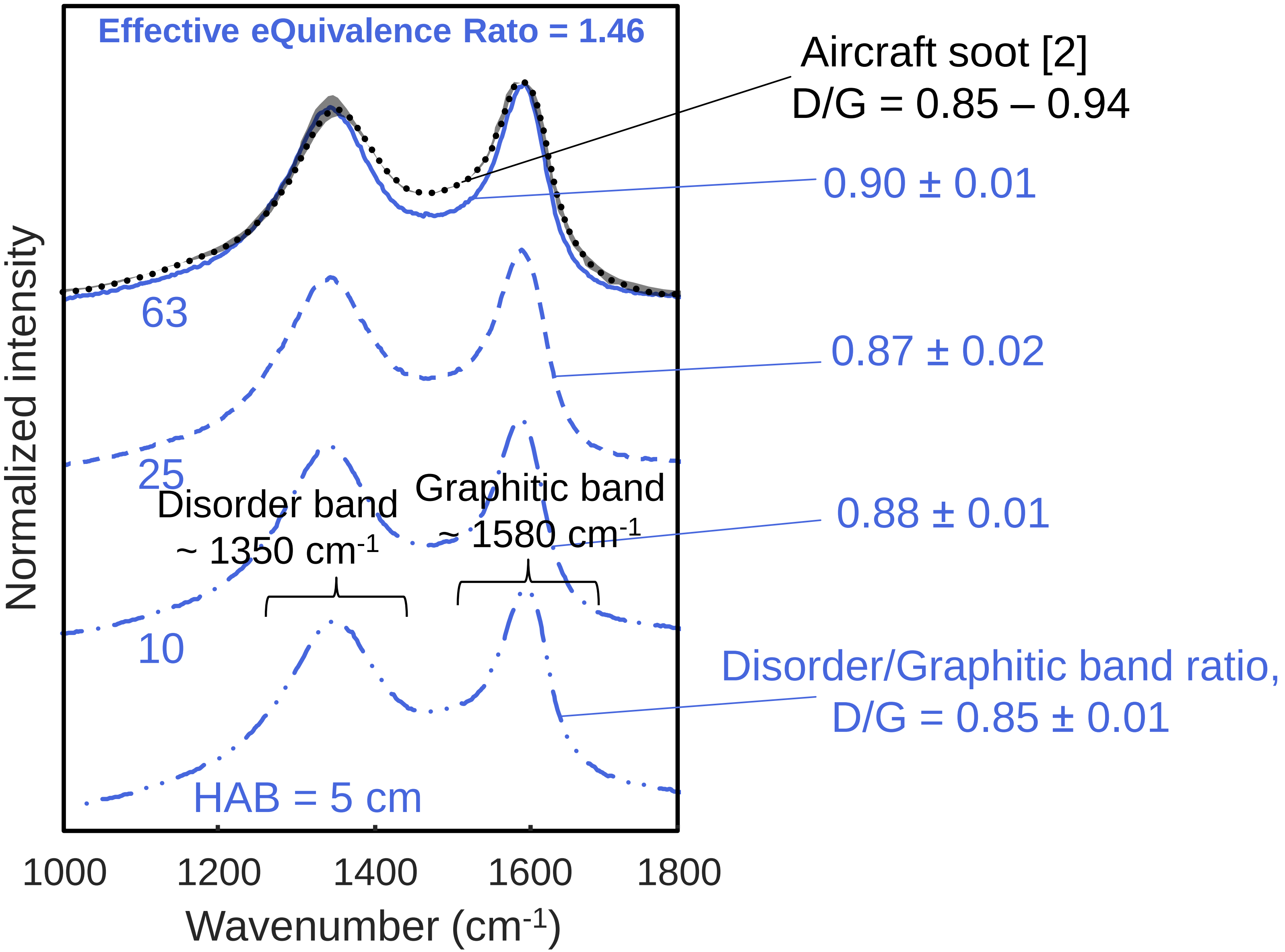

[1] U. Trivanovic, M. Pereira Martins, S. Benz, G.A. Kelesidis, S.E. Pratsinis (2023) *Fuel.* 342, 127864.
[2] P. Parent, C. Laffon, I. Marhaba, D. Ferry, T.Z. Regier, I.K. Ortega, B. Chazallon, Y. Carpentier, C. Forsca (2016) *Carbon.* 101, 86 – 100

Raman D/G ratio vs primary particle diameter

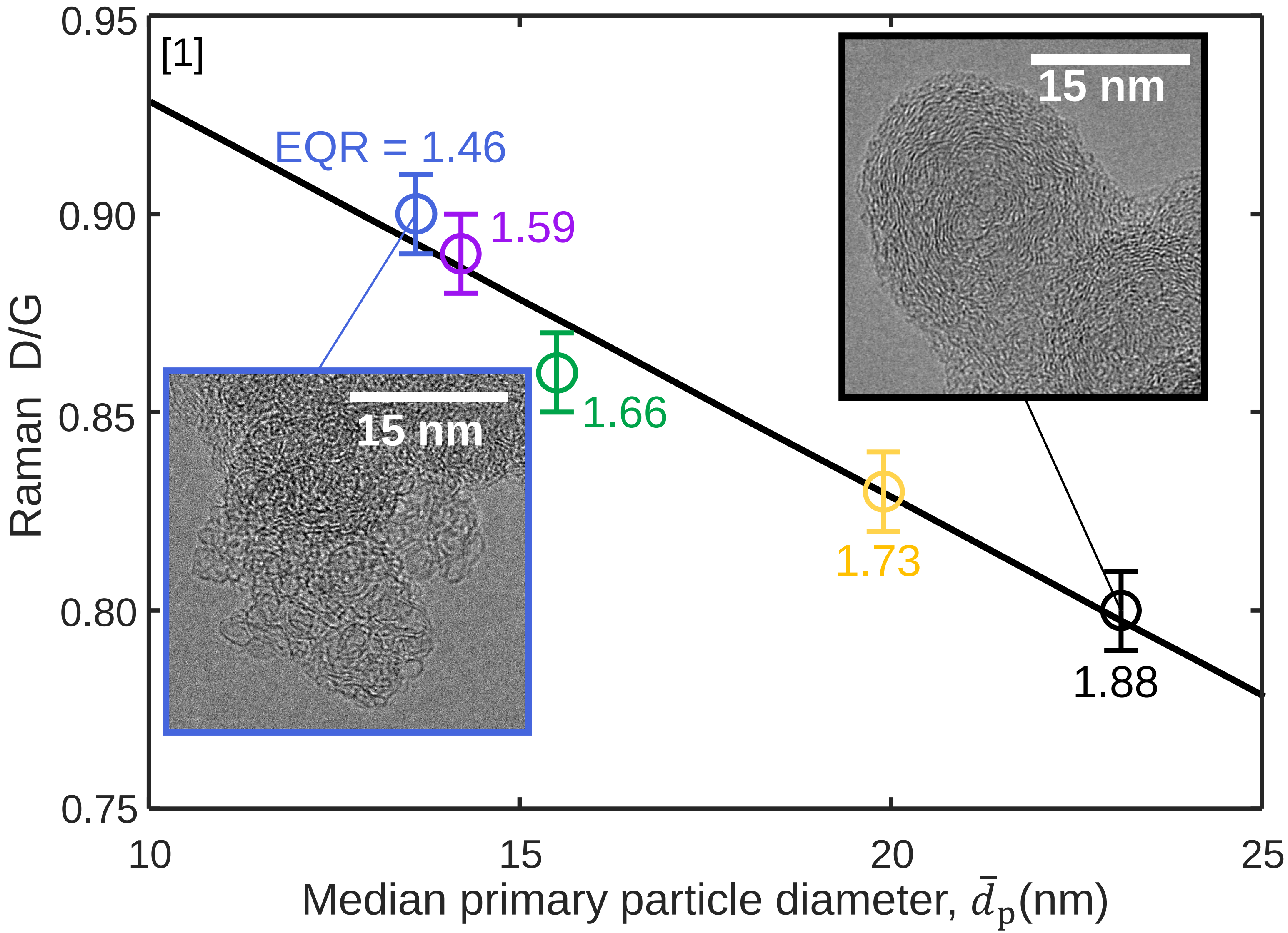

In agreement with size-selected soot from an inverted burner [2] and a gas flare [3].

Meet the Job Seekers Poster 4MJ.8 today at 6pm Exhibit Hall E

[1] U. Trivanovic, M. Pereira Martins, S. Benz, G.A. Kelesidis, S.E. Pratsinis (2023) *Fuel.* 342, 127864.
[2] A. Baldelli, S.N. Rogak (2019) *Atmos. Meas. Tech.* 12, 4339 - 4346
[3] U. Trivanovic, T.A. Sipkens, M. Kazemimanesh, A. Baldelli, A.M. Jefferson, B.M. Conrad, M.R. Johnson, J.C. Corbin, J.S. Olfert, S.N. Rogak (2020) *Fuel 279*, 118478

Crystallite size vs primary particle diameter

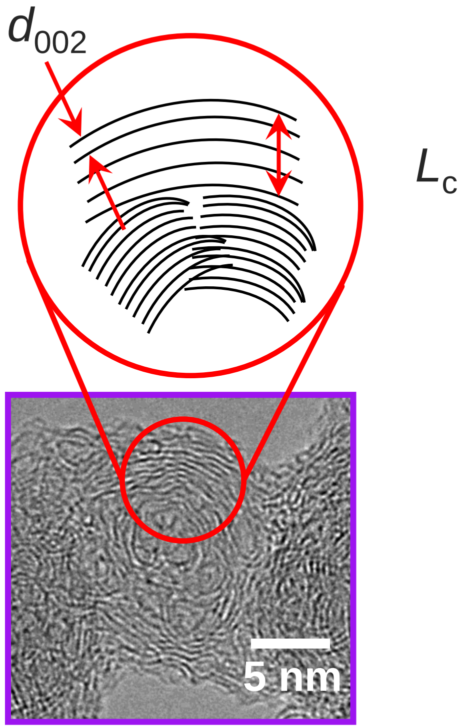

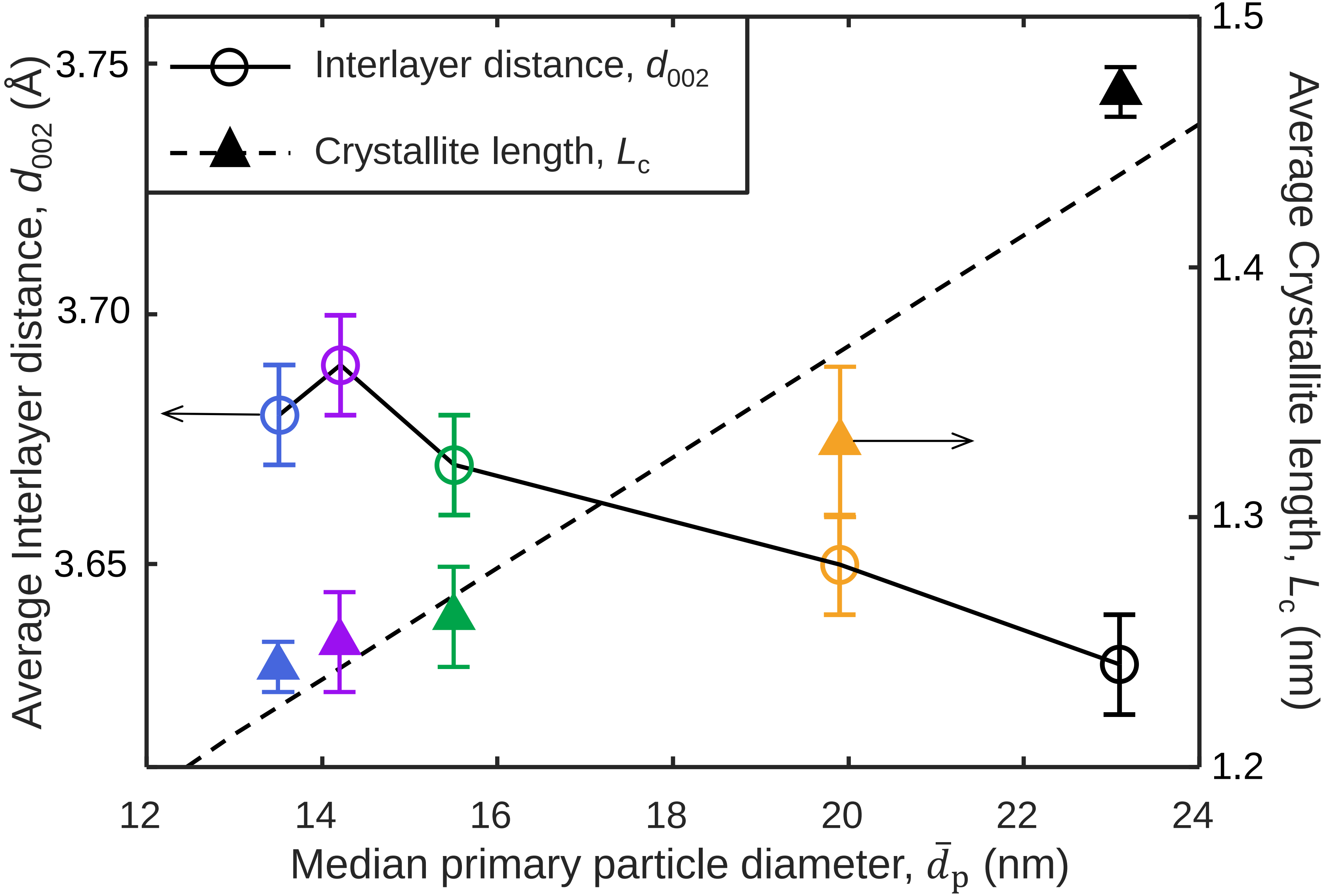

Conclusions

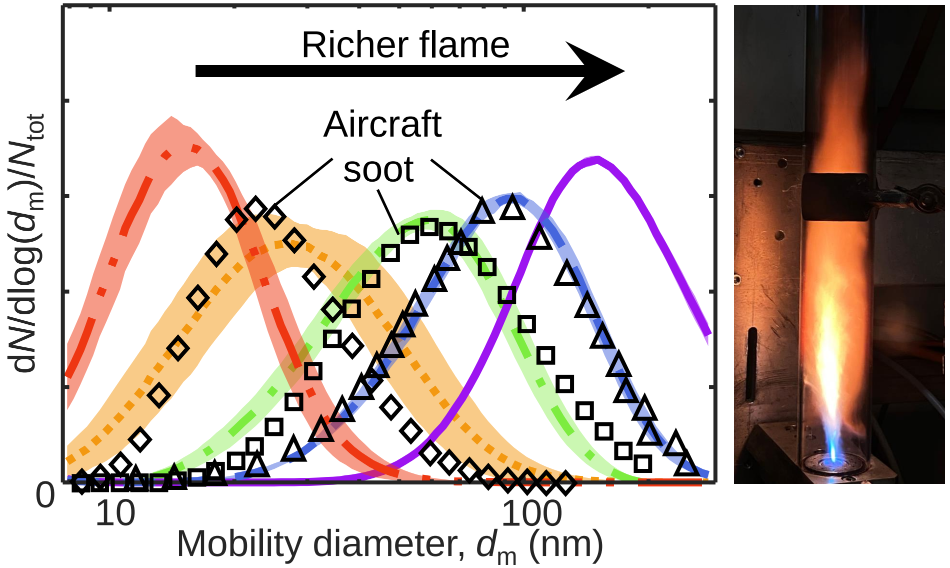

- Relatively large quantities of aircraft-like soot are generated by enclosed spray combustion (ESC)

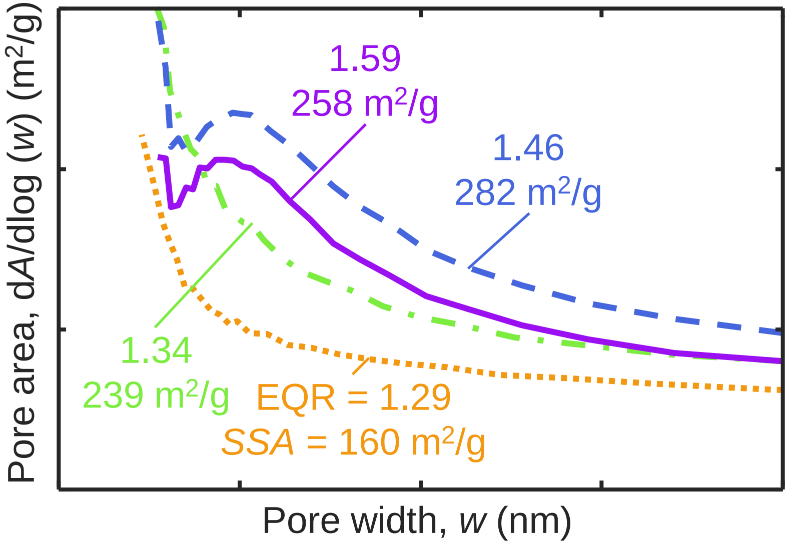

- This allows for example determination of the specific surface area (SSA) showing that such soot is largely non-porous

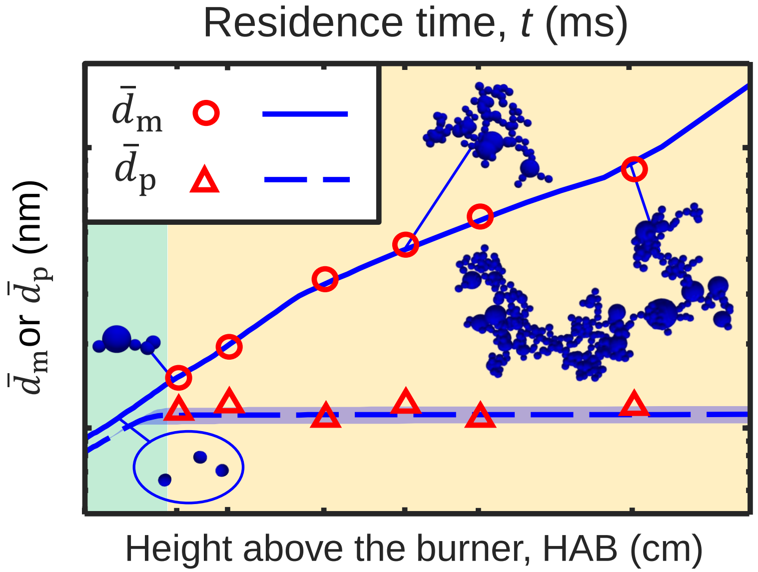

- Soot grows through surface growth for the first few milliseconds and then agglomeration takes over.

U. Trivanovic, G.A. Kelesidis, S.E. Pratsinis (2022) *Aerosol Sci. Technol.* 56, 732-743.
U. Trivanovic, M. Pereira Martins, S. Benz, G.A. Kelesidis, S.E. Pratsinis (2023) *Fuel.* 342, 127864.

Thank you for listening